Reprint from AIP Conference Proceedings 1583 (2014) 24
http://dx.doi.org/10.1063/1.4865597

Influence of the doping on the lattice sites of Fe in Si

D. J. Silva[a], U. Wahl[b], J. G. Correia[b] and J. P. Araújo[a]

[a]*IFIMUP and IN-Institute of Nanoscience and Nanotechnology, Departamento de Física e Astronomia da Faculdade de Ciências da Universidade do Porto, Rua do Campo Alegre 687, 4169-007 Porto,Portugal*
[b]*Instituto Superior Técnico/Instituto Tecnológico e Nuclear, Universidade de Lisboa, -2686-953 Sacavém, Portugal*

Abstract. We report on the lattice location and thermal stability of Fe in n^+- and p^+-type silicon. By means of emission channeling we have observed Fe on ideal substitutional sites, sites located in between bond-centered (BC) and substitutional sites, and sites displaced from tetrahedral towards anti-bonding sites. Here, we focus our analysis on the identification of Fe displaced 0.4-0.6 Å from BC sites and the influence of the doping on the stability of these sites. Fe on near-BC sites is found to be more thermally stable in n^+-type Si than in low doped or p^+-type Si, and seems to be related to multiple vacancy defects. We suggest that the complexes which trap Fe near BC sites, as well as the formation of substitutional Fe, may play a crucial role in P-diffusion gettering.

Keywords: lattice location, emission channeling, Fe in Si, gettering
PACS: 61.72.-y, 61.72.uf, 61.72.Yx, 61.85.+p

INTRODUCTION

The structural and electrical properties of transition metal impurities (TMs) have been an important subject in the manufacturing of Si-based devices. In fact, depending on the complexes that TMs form, deep levels are introduced within the silicon bandgap, which are unwanted in most applications, *e.g.* microelectronics or photovoltaics [1,2]. One of the most harmful TMs is Fe due to its presence in comparatively high concentrations during Si production, *e.g.* iron is present in silica. Gettering has therefore been pointed out as the most effective solution to reduce its malicious effect [3]. Although many gettering procedures have been developed, in particular in solar cell processing P-diffusion (involving n^+ regions) has gained eminence over the past years. The microscopic nature of this gettering mechanism is still not completely clear. It has been suggested, however, that the interaction of Fe with native defects, in particular related to vacancies, might play a role during P-diffusion gettering [4,5,6].

One way to explore the microscopic nature of the interaction of Fe with vacancy-related defects is to study the influence of the doping on the lattice sites of implanted Fe in silicon. A unique technique to investigate the sites of impurities is electron emission channeling (EC) which relies on implanting single crystals with radioactive probe atoms that decay by the emission of β^- particles. The β^- particles experience channeling effects along crystallographic directions depending on the lattice site occupied by the probe atom. EC was previously used to investigate the lattice location of the ^{59}Fe probe atom in different lightly doped Si samples (with resistivities above ~0.01 Ωcm) [7,8]. Three lattice sites were observed: ideal substitutional sites (S), displaced from bond-centered towards substitutional sites (near-BC) and displaced from tetrahedral towards anti-bonding sites (near-T). It seemed, however, that in lightly doped Si the doping was not influencing the preferred lattice sites of implanted Fe, presumably since the defect production during Fe implantation shifts the Fermi level towards midgap, thus compensating the effect of doping.

In this work, we present results on the lattice location of Fe in heavily doped n^+- and p^+-type silicon, with a special focus on the identification and stability of Fe on near-BC sites. A correlation of our findings between the high thermal stability of Fe on near-BC and ideal S sites in n^+-type Si and P-diffusion gettering is given. A more complete description of the experimental results and their comprehensive discussion is about to be published elsewhere [9].

EXPERIMENT

The long-lived isotope ^{59}Fe ($t_{1/2}$ = 44.6 d) was introduced in n^+-type (n^+-Si; resistivity of < 0.001 Ωcm) and p^+-type (p^+-Si; < 0.002 Ωcm) Cz silicon samples by implanting the precursor isotope ^{59}Mn ($t_{1/2}$ = 4.6 s), at the on-line

Reprint from AIP Conference Proceedings 1583 (2014) 24
http://dx.doi.org/10.1063/1.4865597

isotope mass separator facility ISOLDE at CERN, with 60 keV. The fluence was 6×10^{12} cm^{-2}. The depth profiles of the implanted ^{59}Fe and created vacancies were estimated using the SRIM code [10]. The implanted ^{59}Fe profile is approximately a Gaussian distribution centered at 558 Å with a straggling of 213 Å and a peak concentration of 1.1×10^{18} cm^{-3}. At 0 K, each implanted ^{59}Fe creates ~900 vacancies along its path, producing a peak concentration of $\sim5\times10^{21}$ cm^{-3}. The dopants of the n^+- and p^+-Si samples were, respectively, phosphorus and boron. Starting a few days after the implantation, the samples were mounted on a goniometer made of Ta and Mo and annealed in situ up to 900ºC in steps of 100ºC, during 10 min. After each annealing step, the β-emission yield was measured at room temperature using a position and energy-sensitive detector in the vicinity of <110>, <100> and <111> for the n^+-Si and <211>, <100> and <111> for the p^+-Si samples.

RESULTS

The two-dimensional experimental channeling patterns were fitted by using calculated beta emission yields, obtained with the so-called *many beam* formalism for electron channeling in single crystals, in order to quantitatively characterize the occupied lattice sites of ^{59}Fe. The emission probability of the substitutional (S), hexagonal (H), tetrahedral (T), bond-center (BC), anti-bonding (AB), split (SP) and the so-called DS, DT, Y and C sites, as well as <111>, <100> and <110> displacements between these positions were considered in the fitted patterns [11].

In analogy to the previous experiments in low-doped Si [7,8], the same three types of lattice sites (ideal S, near-BC and near-T sites) were necessary to obtain the best fits. As an example, Fig. 1 shows the two-dimensional experimental emission channeling patterns around the <110> direction from as-implanted ^{59}Fe in n^+-Si. Also shown are the calculated emission yields from ideal S, near-BC and near-T sites. Note that the comparatively strong {111} planar channeling in the experimental pattern is a characteristic of the presence of near-BC sites. Also the fact that the axial <110> channeling peak appears spread along the {110} plane indicates that it consists of a superposition of the single peak of ideal S sites and the double peak characteristic for near-BC sites.

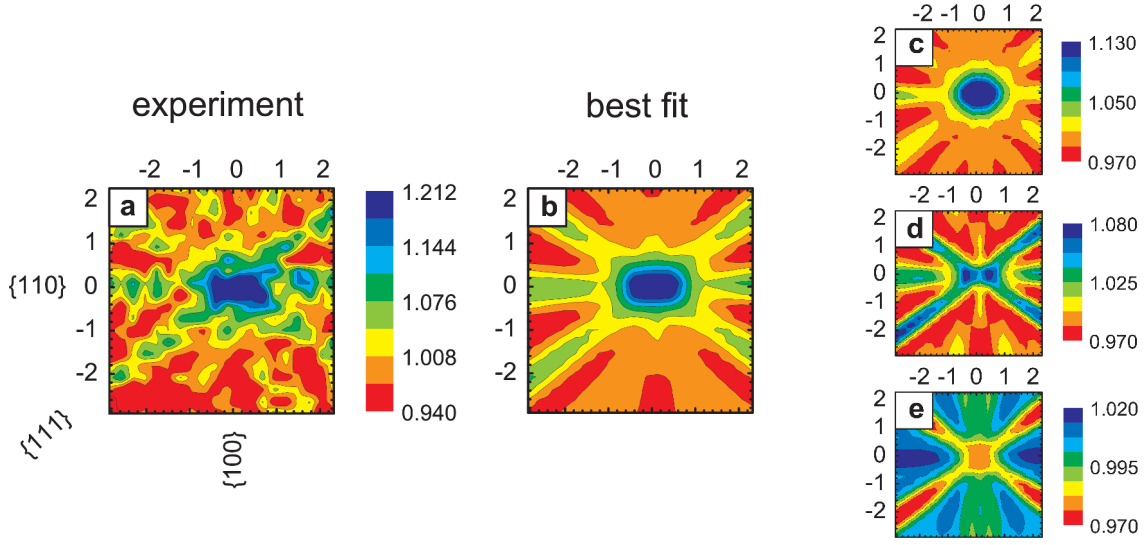

FIGURE 1. Comparison of the **(a)** two-dimensional experimental and **(b)** best fit of theoretical emission channeling patterns from ^{59}Fe in n^+-Si in the vicinity of <110> in the as-implanted state. Panels **(c)**, **(d)** and **(e)** represent the contributions to the EC patterns of the ideal S site (21%), near-BC site (50%) and near-T site (23%) patterns, respectively.

To illustrate in more detail how the occupied lattice sites are identified, we use the determination of the most likely position of Fe in between S and BC sites as an example. In Fig. 2 we plotted for the as-implanted state the reduced χ^2 for multi-site fits as a function of <111> displacements from the ideal positions. In case of the <111> and <100> patterns, the reduced χ^2 is plotted for 2-site fits, where the first site is kept ideally aligned with the <111> or <100> rows (i.e. S or T sites), while the position of the second site is moved along all equivalent <111> directions from the ideally aligned position. One concludes that the position of the second site is roughly around 0.6-0.8 Å from the axis. Note however, that for <111> and <100> patterns the <111> displacements S→BC,

Reprint from AIP Conference Proceedings 1583 (2014) 24
http://dx.doi.org/10.1063/1.4865597

S→AB, T→AB, T→H are completely equivalent, so that these patterns do not allow to independently determine whether the displacement is with respect to S or T sites. In order to distinguish between S or T sites, <110> or <211> patterns are needed (as illustrated already in Fig. 1). In case of the <110> or <211> data in Fig. 2, the reduced χ^2 is plotted for 3-site fits, where the first site is kept fixed at the ideal S position, the second site is kept fixed at a position 0.45 Å from T sites towards AB sites, while the position of the third site is shifted from ideal S towards the BC position as indicated. Note that the exact choice of the interstitial site in this case, e.g. ideal T *vs* a shift from T to AB is not very critical, since the <110> or <211> patterns vary relatively little when the position of the interstitial fraction is varied. Overall, one arrives at the result that the most likely displacement in between S and BC sites is as indicated by the grey shaded area. It is clear from this analysis, that for instance *major* fractions of ^{59}Fe on ideal BC sites can be ruled out, since the χ^2 of fit becomes significantly worse for the <111> patterns, and to lesser extent also for <100> patterns. On the other hand, the possibility of *minor* fractions on ideal BC sites in addition to a *major* displaced fraction exists. To quantitatively assess this possibility it would require performing 3- or 4-site fits. However, in this case the fit results become increasingly ambiguous.

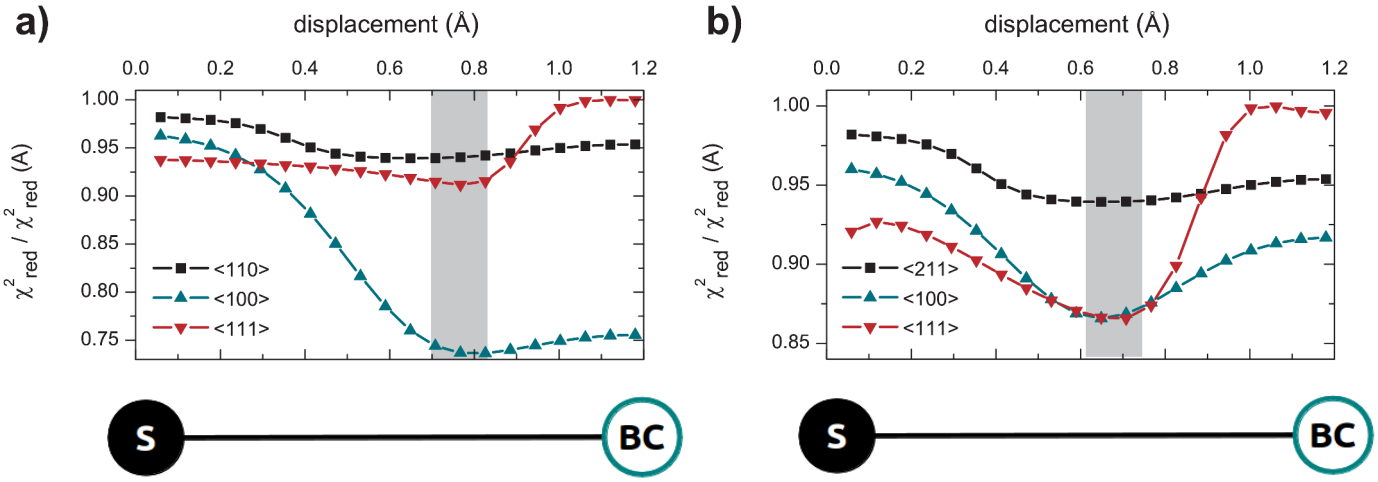

FIGURE 2. Reduced χ^2 of the fits to the experimental emission yields as a function of displacement from ideal S to ideal BC sites following room temperature implantation **(a)** in n^+-Si, for <110>, <100>, and <111>, and **(b)** in p^+-Si for <211>, <100>, and <111>. The reduced chi square $\chi^2_{red}/\chi^2_{red}(A)$ is normalized to single- or double-site fits, where for the <100> and <111> data "A" represents sites ideally aligned with the axis, i.e. ideal S or ideal T, while for the <110> and <211> data "A" represents a combination of ideal S + near-T sites.

Figure 3 shows the annealing temperature dependence of the fractions of ^{59}Fe on the identified lattice sites in n^+- and p^+-Si, in comparison to the average results of low doped Si from Refs. 7-8. While the same three types of lattice sites were identified in analogy to the previous experiments in low-doped Si, the preferred sites of Fe change clearly with the doping of the material. While near-T interstitial sites were dominant in p^+-Si (~91% after annealing at 400ºC), the majority of Fe occupied near-BC sites in n^+-Si (~65 % after annealing at 500ºC).

DISCUSSION AND CONCLUSION

Comparing these EC experiments with theoretical predictions, one concludes that the ideal S and near-BC sites result from the interaction of iron with vacancy-type defects. In fact, ab-initio calculations have shown that Fe prefers ideal S sites when trapped by single vacancies, while divacancies should trap iron on ideal BC sites [12]. What cannot be explained so far by theory is the displacement of Fe from the ideal BC site towards S sites suggested by our data. It seems, however, feasible that the near-BC fraction represents a mixture of Fe not only inside divacancies but also inside more complicated multivacancies where it may sit somewhat off the ideal BC site, e.g. inside multivacancies with fourfold configurations based on hexavacancy rings [13,14].

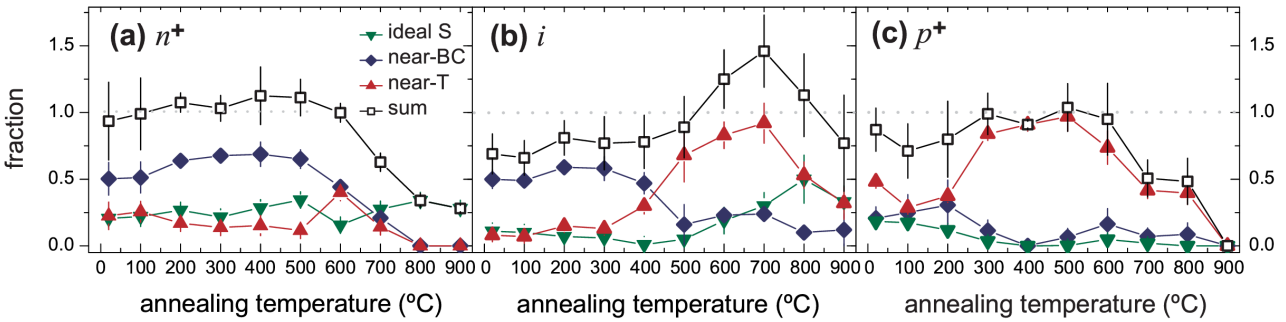

FIGURE 3. Annealing temperature dependence of the ideal S, near-BC and near-T fractions in n^+-Si, p^+-Si, and low doped silicon (i-Si). Data for i-Si are from Refs. 7-8.

As is discussed in detail in Ref. [9], the microscopic nature of the near-T sites in p^+-Si is not totally clear at the moment, although the positive charge state of interstitial Fe_i^+ in p^+-Si and the formation of Fe^+B^- pairs are obviously expected to play a major role. In that respect it seems that the sites of Fe within Fe^+B^- pairs are substantially displaced (up to 0.5 Å) from the ideal T site towards the AB site. While this would agree with the lattice site estimated from the measured pair binding energy of 0.65 eV found in the literature, assunming a simple Coulomb interaction between Fe^- and B^+, it is not obvious to reconcile it with the structure of the Fe^+B^- pair predicted by ab-initio calculations, consisting of Fe on an ideal T site with a breathing mode relaxation (0.27 Å inward) of the four Si atoms surrounding the B atom [15].

To conclude, we have studied the influence of n^+ and p^+ doping on the lattice sites of implanted iron in silicon. While near-T interstitial sites are prominent in p^+-type silicon, Fe clearly prefers near-BC sites in n^+-type silicon. Arguments have been given to support that near-BC sites result from the trapping of Fe into multivacancy defects produced during implantation. We have shown that the thermal stability of near-BC Fe is higher in n^+- than in low doped or p^+-Si. Remarkably, following annealing at 500°C more than 90% of Fe in n^+-Si remains trapped in vacancy-related complexes, i.e. in near-BC or ideal S-sites. We hence propose that the strong interaction with vacancy-type defects and the thermally stable binding of Fe to them, both of which are characteristic for n^+-Si, play a crucial role in the P-diffusion gettering process, where Fe is gettered in the n^+-doped surface region created during the in-diffusion of phosphorus.

ACKNOWLEDGMENTS

This work was supported by ”Fundação para a Ciência e a Tecnologia” - FCT, Portugal (project CERN-FP-123585-2011) and by the European Commission 7th Framework through ENSAR (European Nuclear Science and Applications Research, Contract No. 262010). D.J. Silva is thankful for FCT Grant (SFRH/BD/69/435/2010). The ISOLDE collaboration, in particular the technical team, is acknowledged for providing radioactive ^{59}Mn beams.

REFERENCES

1. E. R. Weber, *Appl. Phys. A* **30**, 1 (1983).
2. A. A. Istratov, H. Hieslmair, and E. R. Weber, *Appl. Phys. A* **69**, 13 (1999).
3. S. M. Myers, M. Seibt, and W. Schröter, *J. Appl. Phys*. **88**, 3795 (2000).
4. A. Bentzen and A. Holt, *Mater. Sci. Eng. B-Adv. Funct. Solid State Mater.* **159-160**, 228 (2009).
5. S. P. Phang and D. MacDonald, *J. Appl. Phys*. **109**, 073521 (2011).
6. M. Syre, S. Karazhanov, B. R. Olaisen, A. Holt, and B. G. Svensson, *J. Appl. Phys*. **110**, 024912 (2011).
7. U. Wahl, J. G. Correia, E. Rita, J. P. Araújo, and J. C. Soares, *Phys. Rev. B* **72**, 014115 (2005).
8. U. Wahl, J. G. Correia, E. Rita, J. P. Araújo, and J. C. Soares, *Nucl. Instrum. Methods Phys. Res. B* **253**, 167 (2006).
9. D. J. Silva, U. Wahl, J. G. Correia, and J. P. Araújo, *J. Appl. Phys.* **115**, 023504 (2014).
10. J. F. Ziegler, *Nucl. Instrum. Methods Phys. Res. B* **219-220**, 1027 (2004).
11. U. Wahl, J. G. Correia, A. Vantomme, and G. Langouche, *Phyica B* **273-274**, 367 (1999).
12. S. K. Estreicher, M. Sanati, and N. G. Szwacki, *Phys. Rev. B* **77**, 125214 (2008).
13. D. V. Makhov and L. J. Lewis, *Phys. Rev. Lett.* **92**, 255504 (2004).
14. S. K. Estreicher, *Phys. Rev. B* **60**, 5375 (1999).
15. M. Sanati, N. G. Szwacki, and S. K. Estreicher, *Phys. Rev. B* **76**, 125204 (2007).